

Figure 1. General location map of the North Slope of Alaska showing the location of NPR, related oil and gas fields, and selected geologic provinces. Modified from (Kumar, Bird, and others, 2002) .

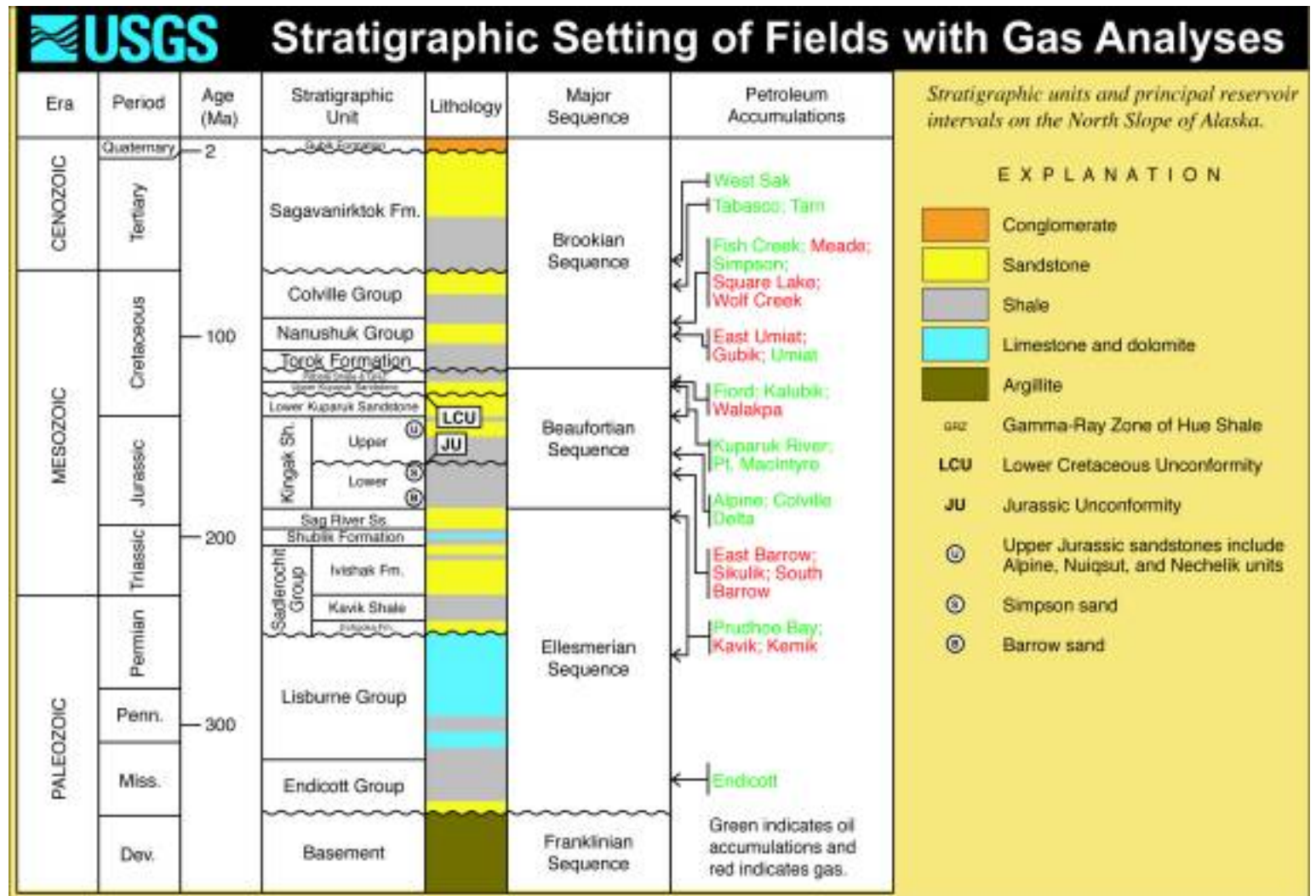


Figure 2. Stratigraphic chart showing major reservoir rock units within and adjacent to NPRA. The stratigraphic intervals of the known oil and gas accumulations discussed in this paper are indicated. Modified from (Kumar, Bird, and others, 2002) .

Figure 3A

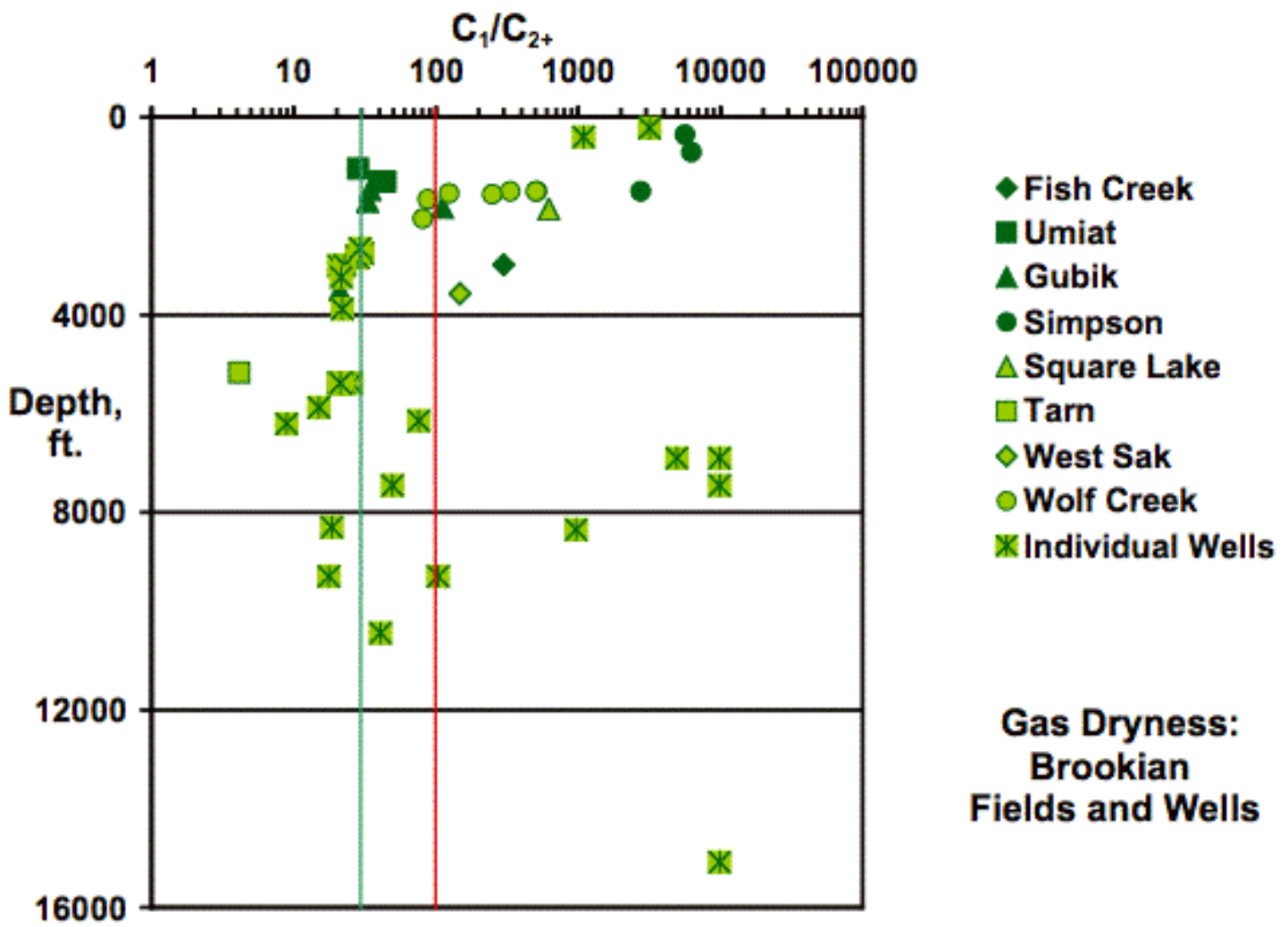


Figure 3. The hydrocarbon composition, shown as gas dryness, C_1/C_{2+} , plotted as a function of depth for the three major stratigraphic sequences on the North Slope. 3A: Brookian reservoirs (green), 3B: Beaufortian reservoirs (blue), 3C: Ellesmerian reservoirs (red). Subsequent figures will use this color coding to distinguish samples from different stratigraphic sequences. Samples are from wells in known fields and individual wells outside of known accumulations. In each plot, vertical red and green lines mark C_1/C_{2+} ratios of 100 (approx. 1% C_{2+}) and 30 (approximately 3% C_{2+}), respectively.

Figure 3B

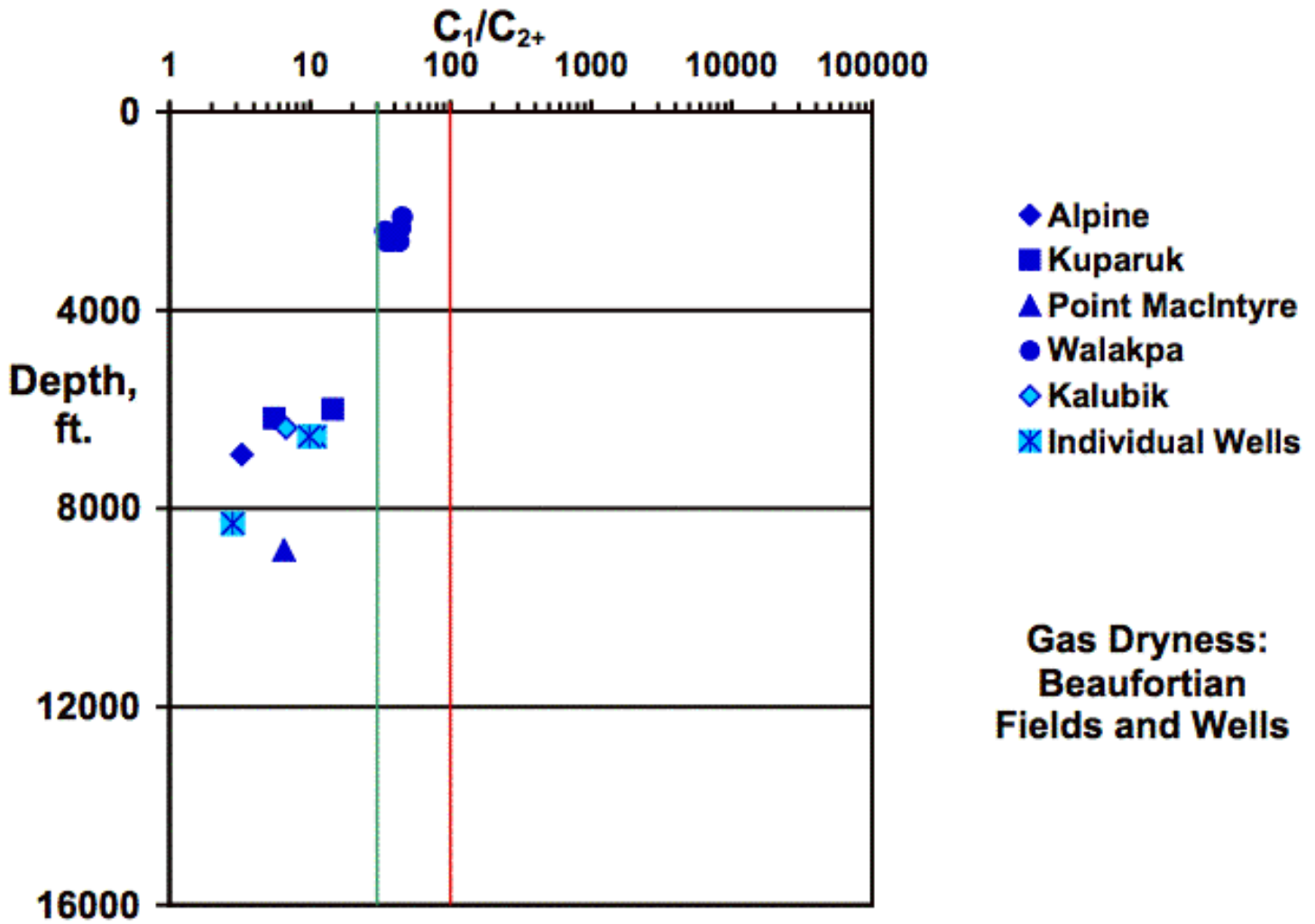


Figure 3. The hydrocarbon composition, shown as gas dryness, C_1/C_{2+} , plotted as a function of depth for the three major stratigraphic sequences on the North Slope. 3A: Brookian reservoirs (green), 3B: Beaufortian reservoirs (blue), 3C: Ellesmerian reservoirs (red). Subsequent figures will use this color coding to distinguish samples from different stratigraphic sequences. Samples are from wells in known fields and individual wells outside of known accumulations. In each plot, vertical red and green lines mark C_1/C_{2+} ratios of 100 (approx. 1% C_{2+}) and 30 (approximately 3% C_{2+}), respectively.

Figure 3C

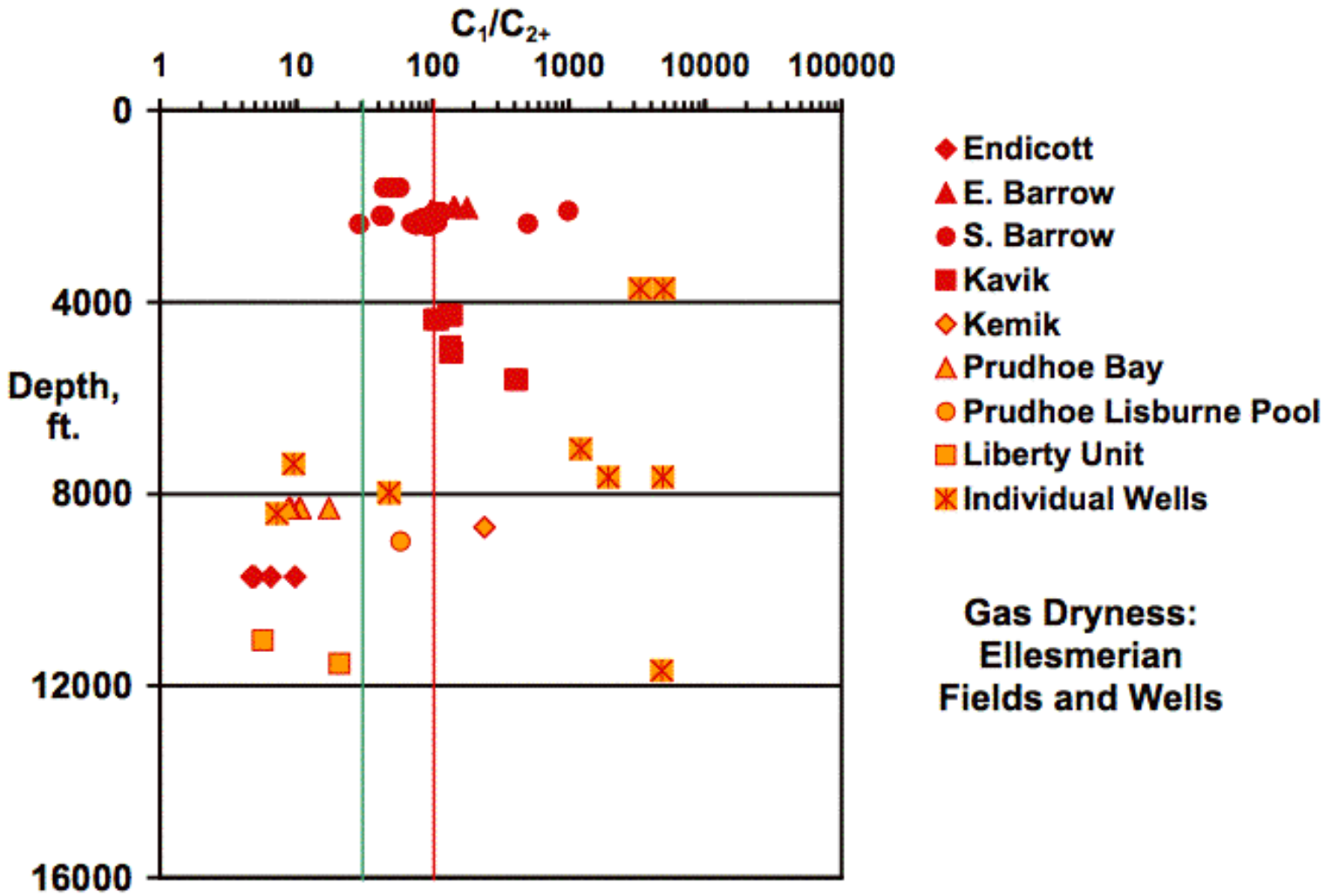


Figure 3. The hydrocarbon composition, shown as gas dryness, C_1/C_{2+} , plotted as a function of depth for the three major stratigraphic sequences on the North Slope. 3A: Brookian reservoirs (green), 3B: Beaufortian reservoirs (blue), 3C: Ellesmerian reservoirs (red). Subsequent figures will use this color coding to distinguish samples from different stratigraphic sequences. Samples are from wells in known fields and individual wells outside of known accumulations. In each plot, vertical red and green lines mark C_1/C_{2+} ratios of 100 (approx. 1% C_{2+}) and 30 (approximately 3% C_{2+}), respectively.

Figure 4A

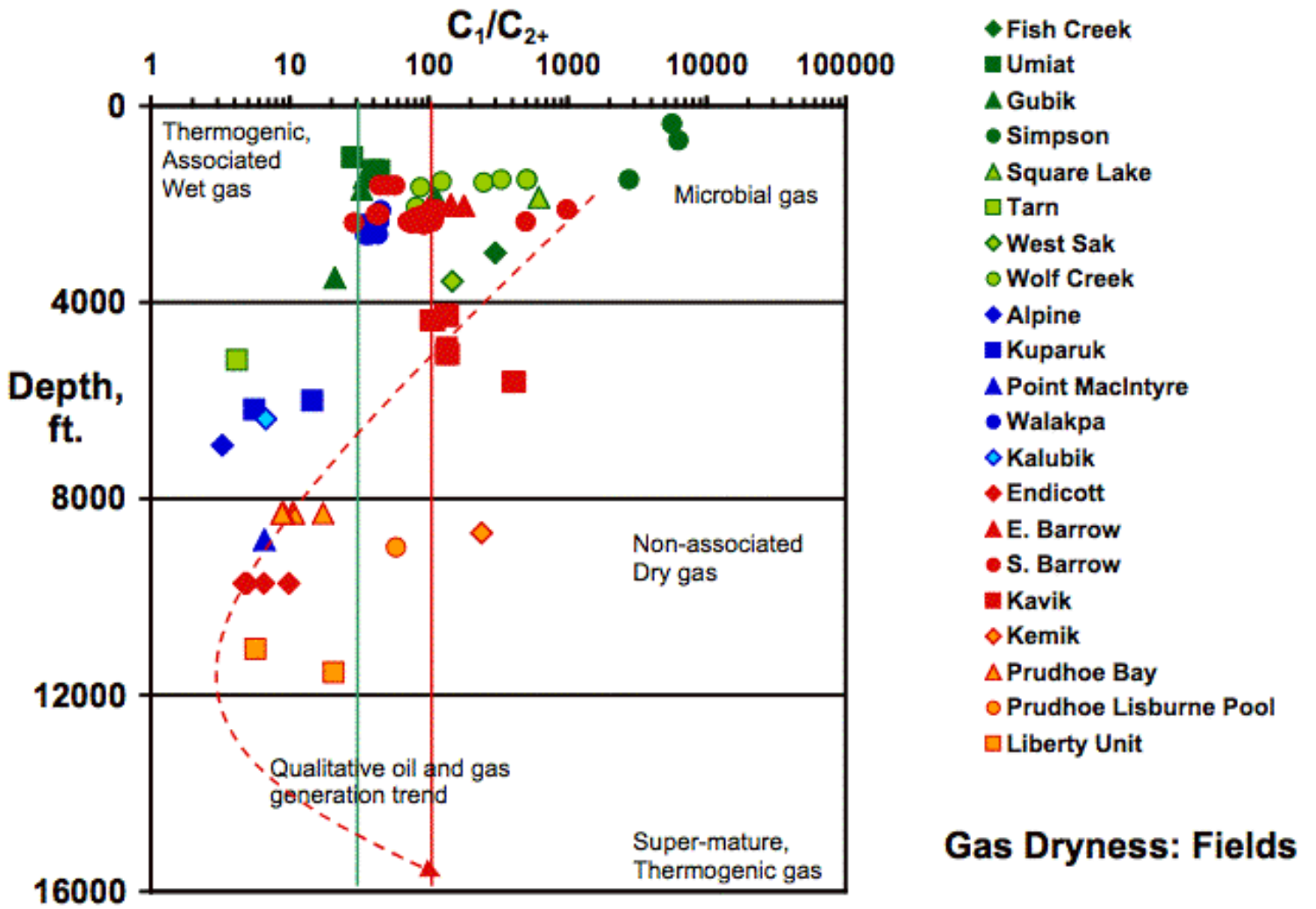


Figure 4. The hydrocarbon composition, shown as gas dryness, C_1/C_{2+} , plotted as a function of depth for known oil and gas fields (4A) and all samples including fields and individual wells outside of known accumulations (4B). Color coding as in Figure 3..

Figure 4B

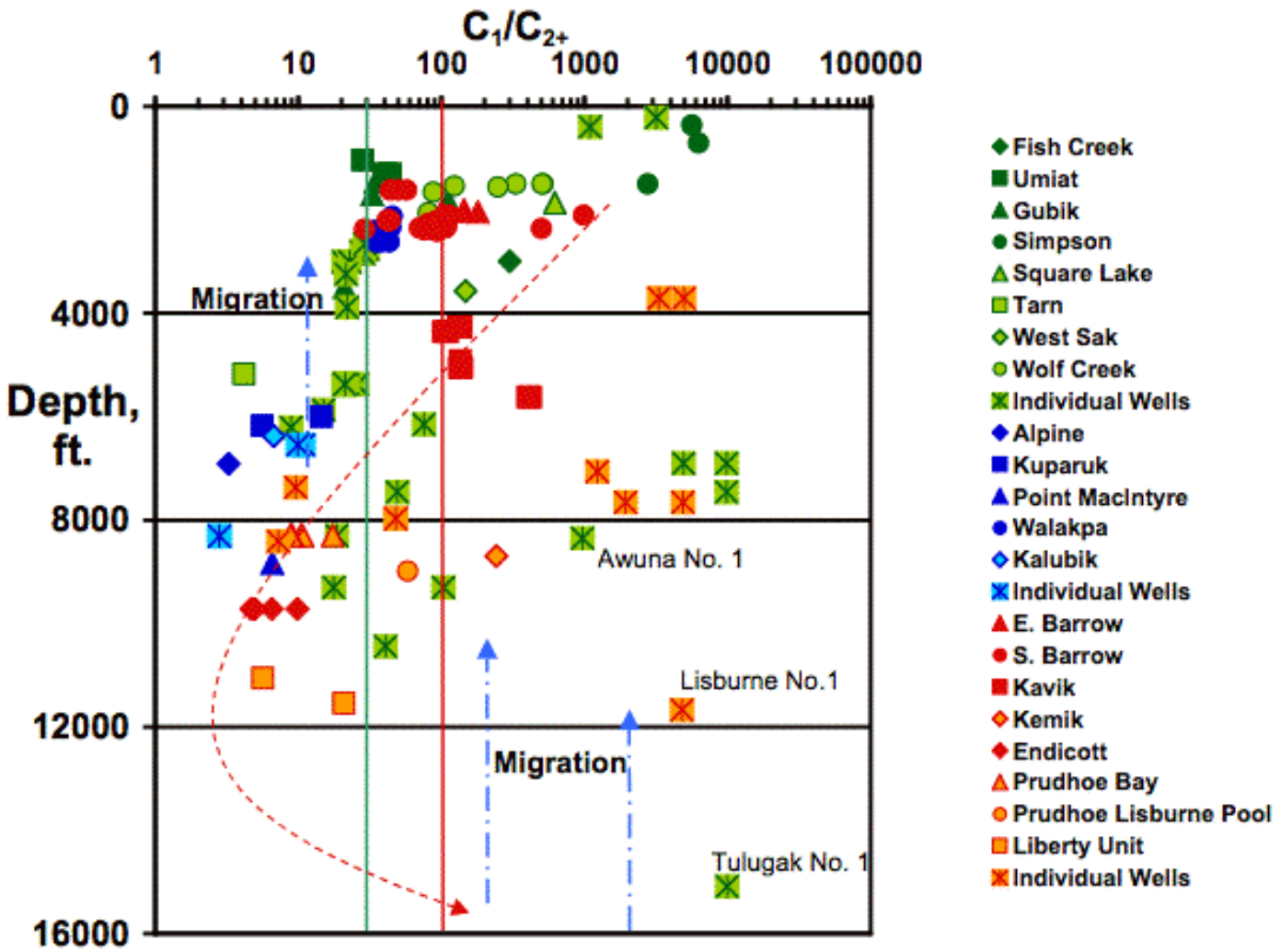


Figure 4. The hydrocarbon composition, shown as gas dryness, C_1/C_{2+} , plotted as a function of depth for known oil and gas fields (4A) and all samples including fields and individual wells outside of known accumulations (4B). Color coding as in Figure 3..

Figure 5A

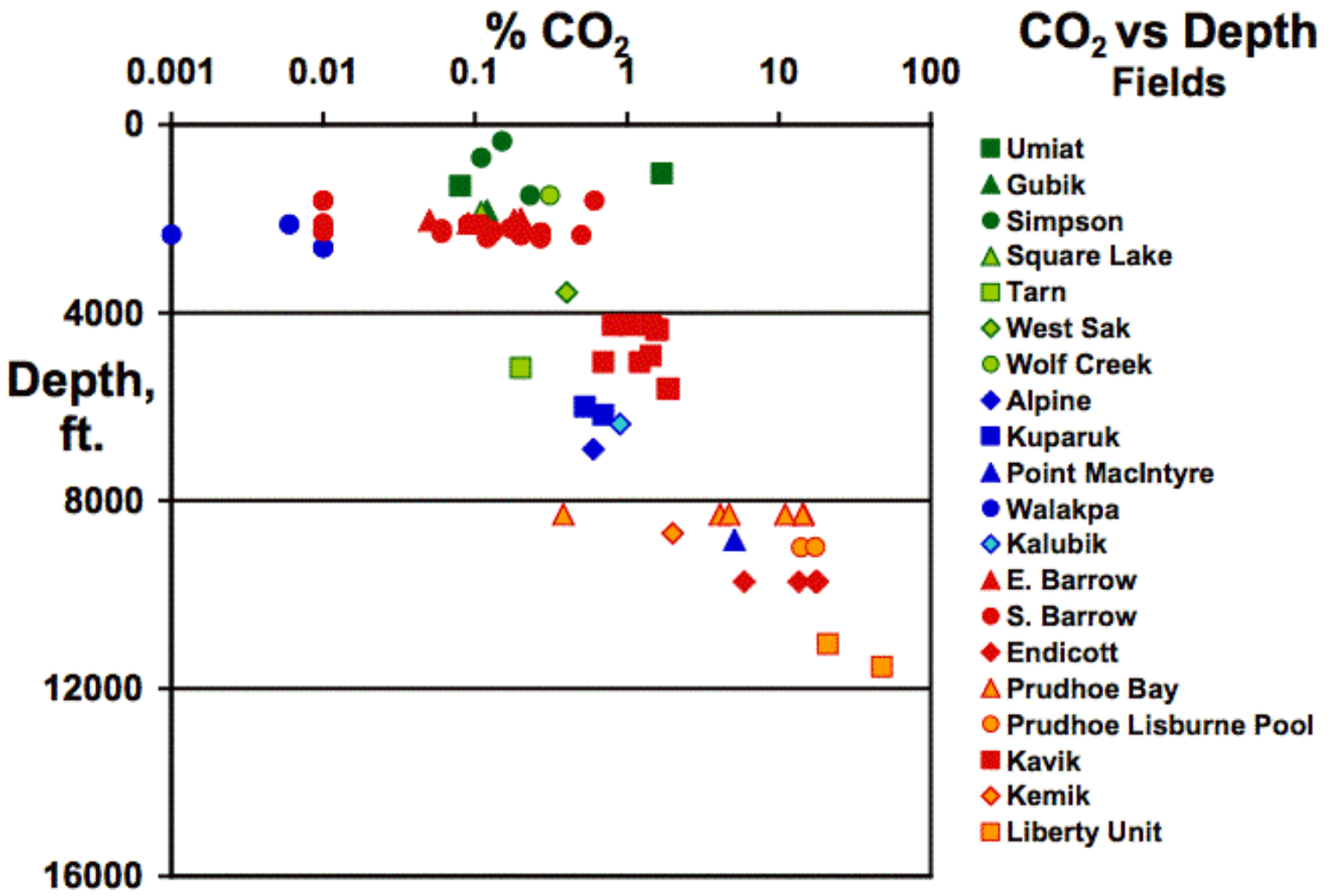


Figure 5. The CO₂ content of North Slope gases as a function of depth, stratigraphic sequence, and the occurrence of samples within known fields (5A) and all samples including non-field wells (5B).

Figure 5B

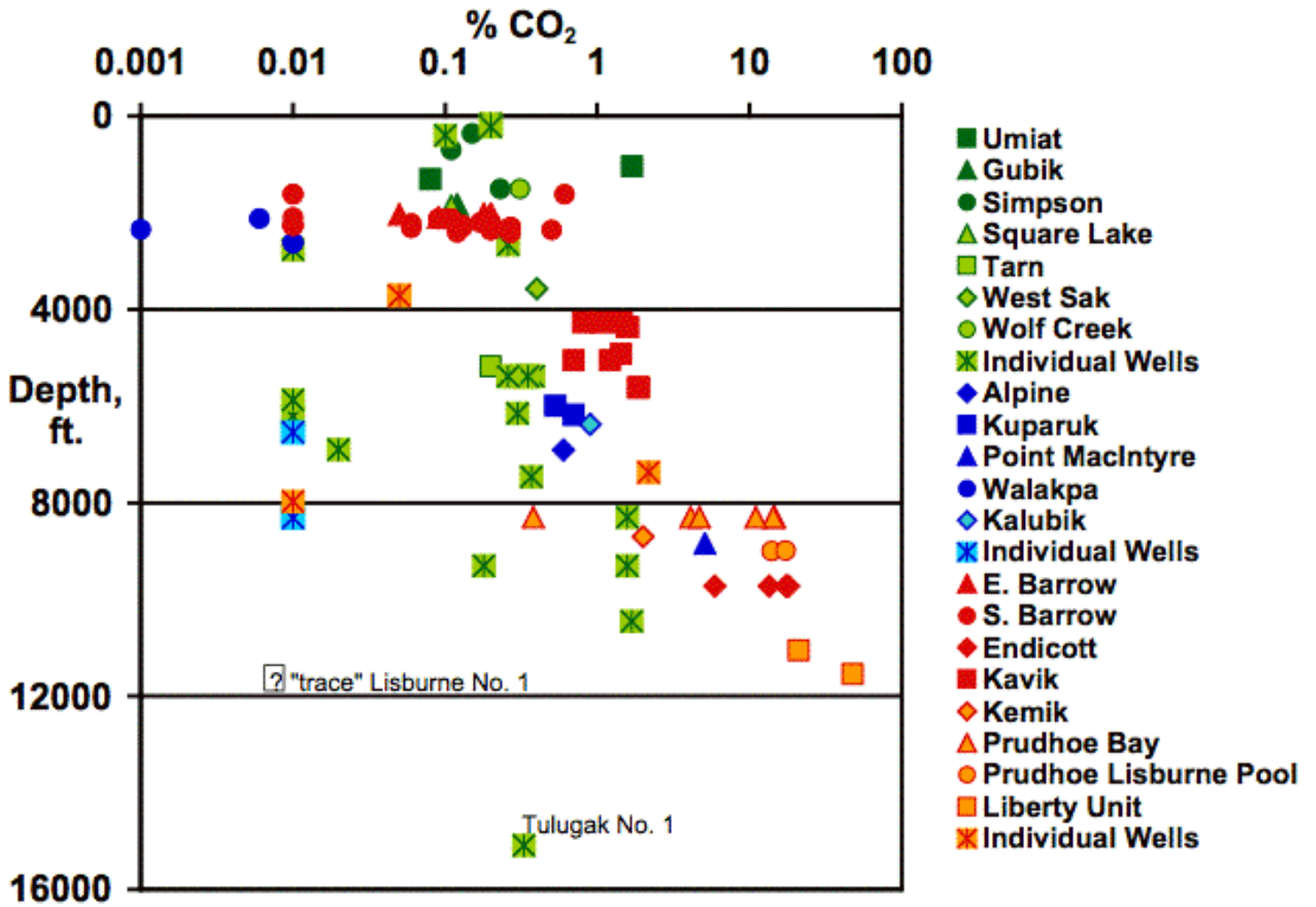


Figure 5. The CO₂ content of North Slope gases as a function of depth, stratigraphic sequence, and the occurrence of samples within known fields (5A) and all samples including non-field wells (5B).

Figure 6

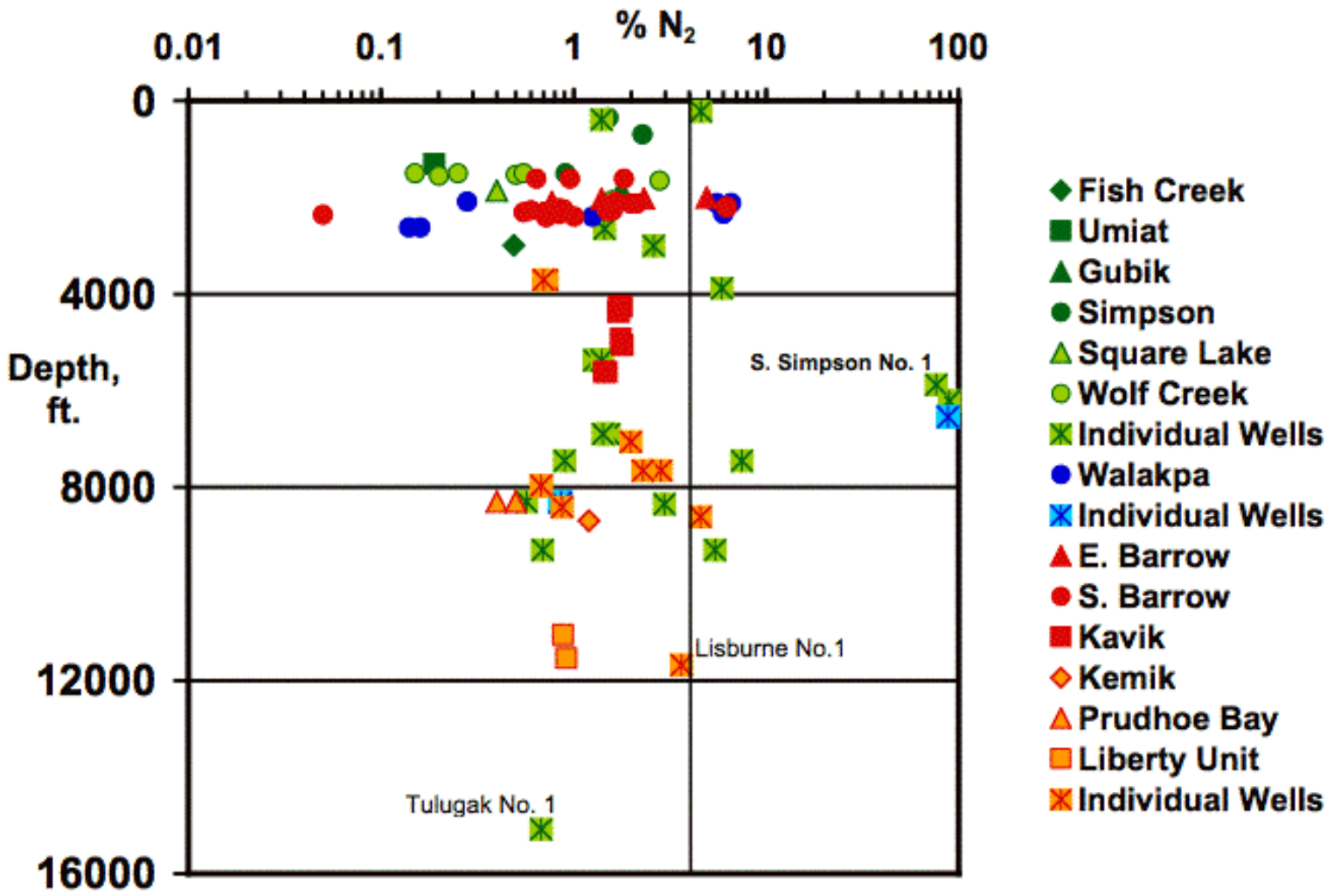


Figure 6. The N₂ content of North Slope gases as a function of depth, stratigraphic sequence, and the occurrence of samples within known fields or in non-field wells. The vertical line at 4 mole % N₂ provides a visual reference to distinguish high N₂ content samples from the more frequent low values that are typical of oil field gases.

Figure 7

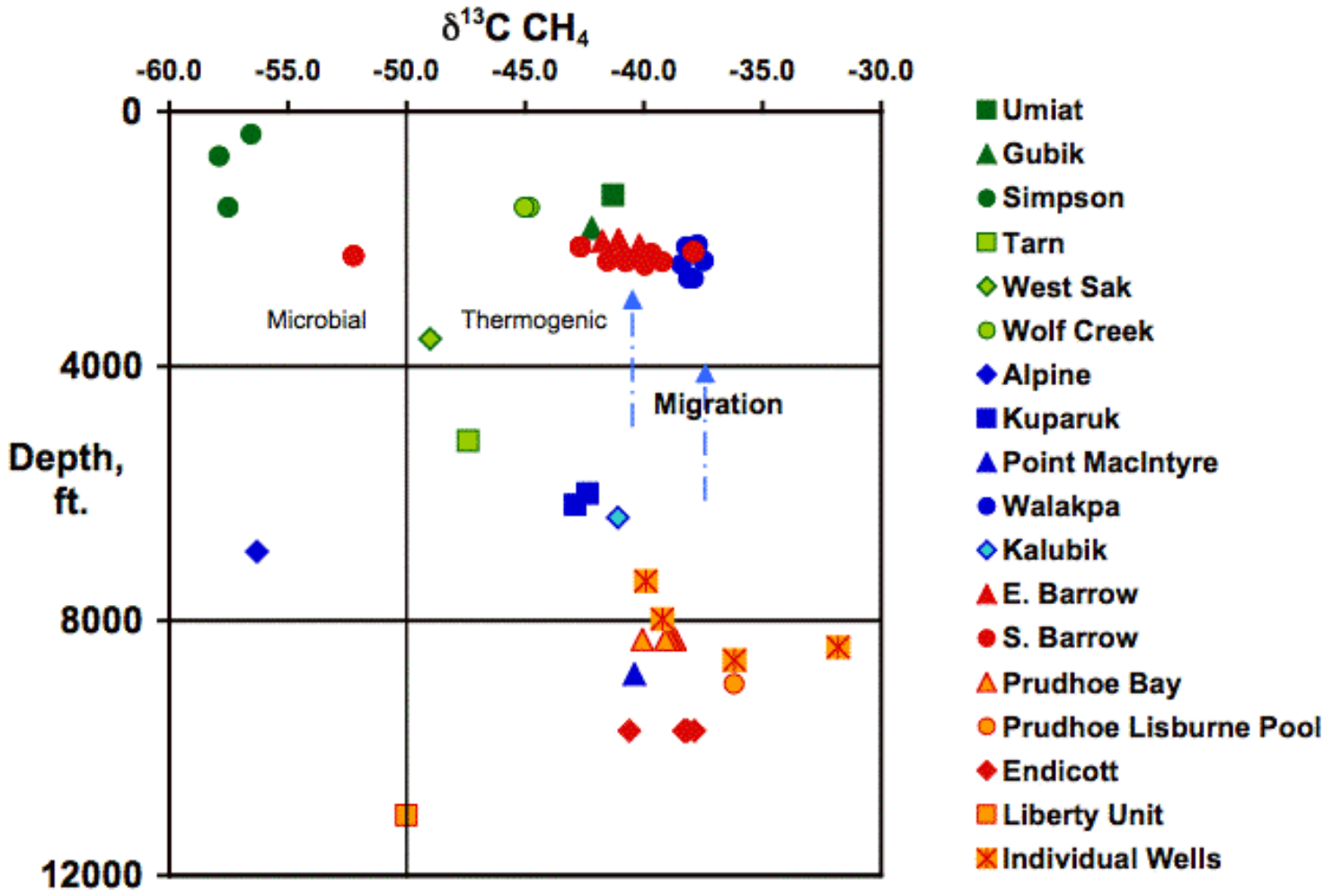


Figure 7. Carbon isotopic composition of methane as a function of depth with samples color coded for stratigraphic sequence of the reservoir.

Figure 8

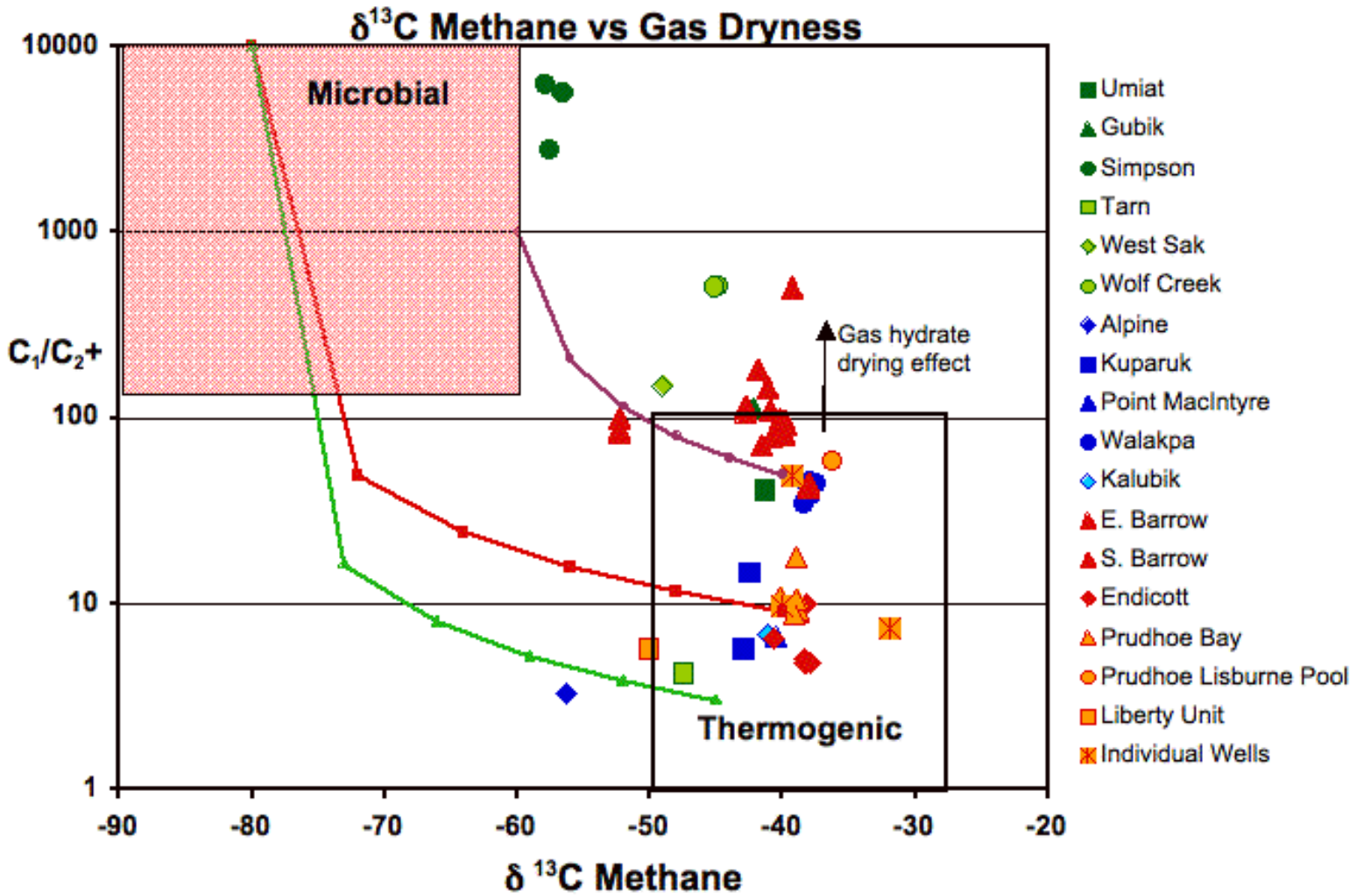


Figure 8. Carbon isotopic composition of methane as a function of hydrocarbon gas composition, shown as gas dryness, C_1/C_{2+} . Fields are labeled to show the range of values expected for methane generated by microbial processes and thermogenic cracking reactions. Curving lines are hypothetical mixing models that show the range of compositions that can occur due to mixing between microbial and thermogenic endmembers. The magenta curve is a hypothetical mixing line between a “Simpson-like” endmember and a “Prudhoe Gas Cap” type endmember. The red curve is the mixing line between a very light and dry microbial gas and a less mature “Prudhoe-like” endmember. The green curve is a mixing line between the light microbial endmember and a very wet, low thermal maturity gas. The vertical line shows the possible effects of gas hydrate formation on the gas composition in shallow reservoirs beneath and within permafrost.

Figure 9

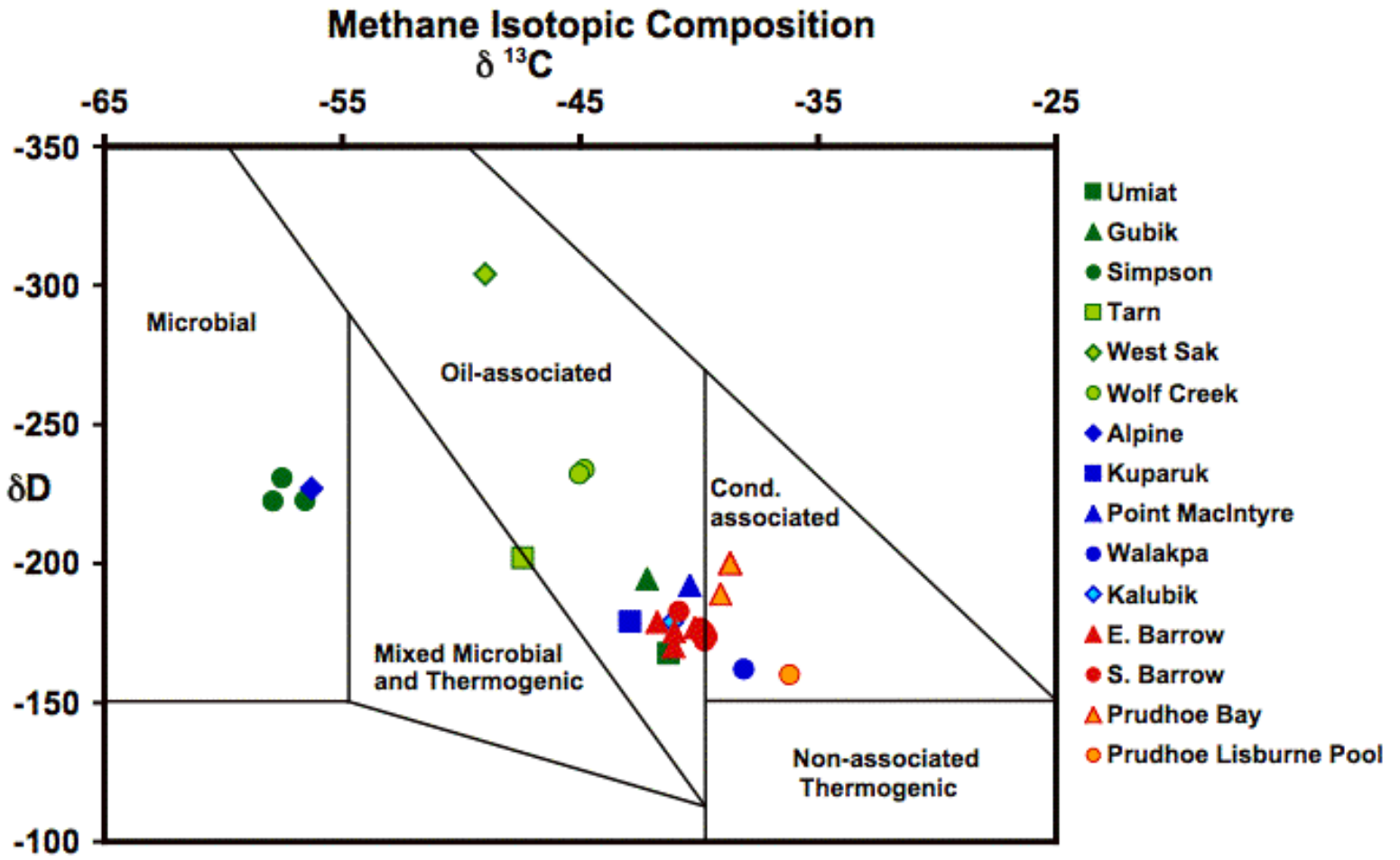


Figure 9. The carbon and hydrogen isotopic composition of methane with fields labeled according to Schoell (Schoell, 1983) .

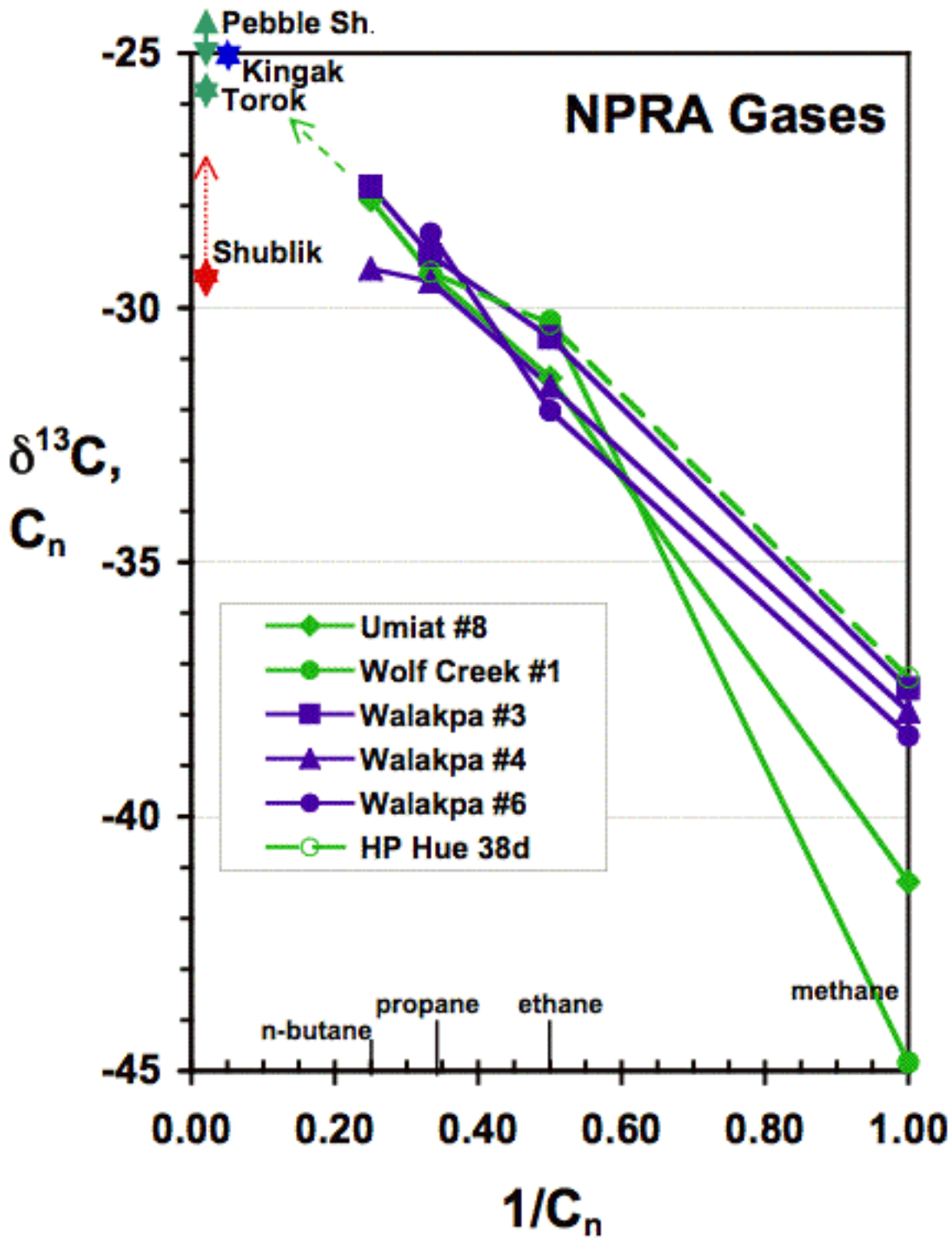


Figure 10. The natural gas plot (Chung, Gormly, and Squires, 1988) showing the carbon isotopic composition of individual hydrocarbons as a function of the carbon number (C_n) of the hydrocarbon. Gases from Walakpa, Wolf Creek, and Umiat fields and one laboratory generated gas from the Hue Shale (see Figure

10E) are shown in 10A. Ranges of the carbon isotopic composition of kerogen from the Shublik Formation, Kingak Shale, Torok Formation shales, and the Pebble shale unit are shown adjacent to the y-axis. Data are from (Burwood, Cole, and others, 1985; Schoell, Wehner, and Coleman, 1985) . Figure 10B shows gases from the South Barrow and East Barrow fields. Gases from the greater Prudhoe Bay area are shown in figure 10C. Additional gases from the greater Prudhoe Bay area and the adjacent fields on the western edge of the greater Kuparuk River field (Masterson, 2001) are shown in 10D. Gases generated in the laboratory during hydrous pyrolysis of North Slope source rocks are shown in Figure 10E. See text for discussion.

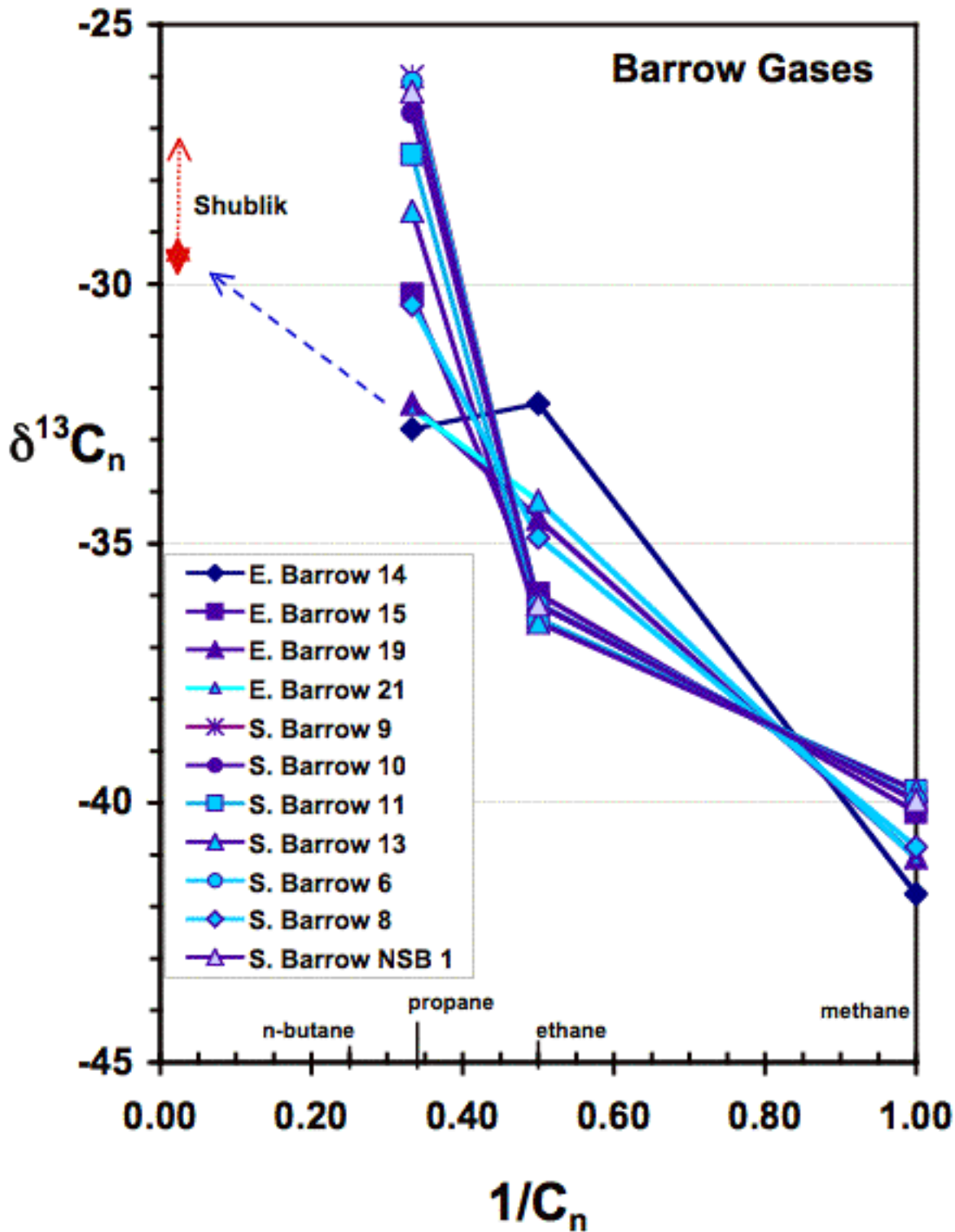


Figure 10. The natural gas plot (Chung, Gormly, and Squires, 1988) showing the carbon isotopic composition of individual hydrocarbons as a function of the carbon number (C_n) of the hydrocarbon. Gases from Walakpa, Wolf Creek, and Umiat fields and one laboratory generated gas from the Hue Shale (see Figure

10E) are shown in 10A. Ranges of the carbon isotopic composition of kerogen from the Shublik Formation, Kingak Shale, Torok Formation shales, and the Pebble shale unit are shown adjacent to the y-axis. Data are from (Burwood, Cole, and others, 1985; Schoell, Wehner, and Coleman, 1985) . Figure 10B shows gases from the South Barrow and East Barrow fields. Gases from the greater Prudhoe Bay area are shown in figure 10C. Additional gases from the greater Prudhoe Bay area and the adjacent fields on the western edge of the greater Kuparuk River field (Masterson, 2001) are shown in 10D. Gases generated in the laboratory during hydrous pyrolysis of North Slope source rocks are shown in Figure 10E. See text for discussion.

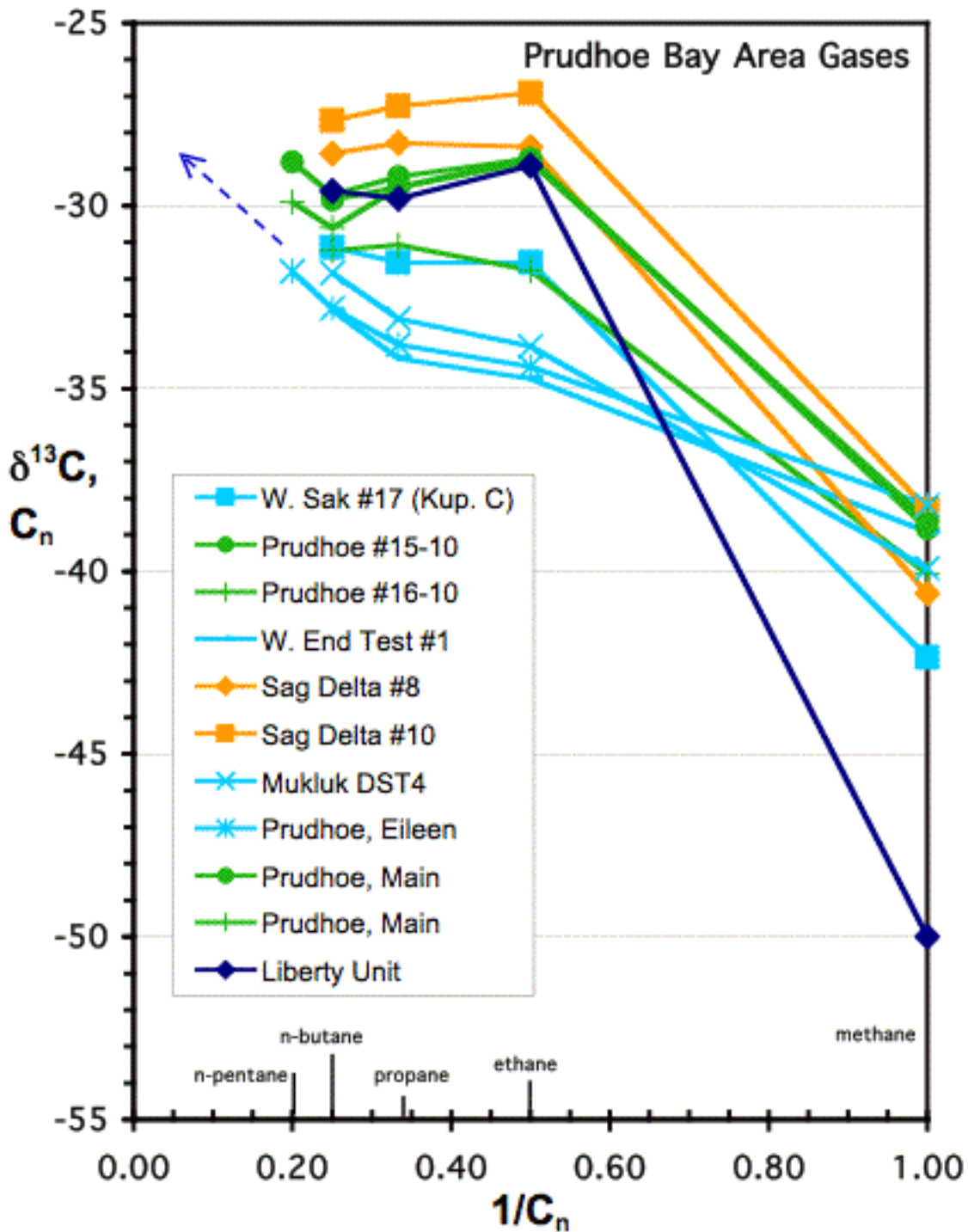


Figure 10. The natural gas plot (Chung, Gormly, and Squires, 1988) showing the carbon isotopic composition of individual hydrocarbons as a function of the carbon number (C_n) of the hydrocarbon. Gases from Walakpa, Wolf Creek, and Umiat fields and one laboratory generated gas from the Hue Shale (see Figure

10E) are shown in 10A. Ranges of the carbon isotopic composition of kerogen from the Shublik Formation, Kingak Shale, Torok Formation shales, and the Pebble shale unit are shown adjacent to the y-axis. Data are from (Burwood, Cole, and others, 1985; Schoell, Wehner, and Coleman, 1985) . Figure 10B shows gases from the South Barrow and East Barrow fields. Gases from the greater Prudhoe Bay area are shown in figure 10C. Additional gases from the greater Prudhoe Bay area and the adjacent fields on the western edge of the greater Kuparuk River field (Masterson, 2001) are shown in 10D. Gases generated in the laboratory during hydrous pyrolysis of North Slope source rocks are shown in Figure 10E. See text for discussion.

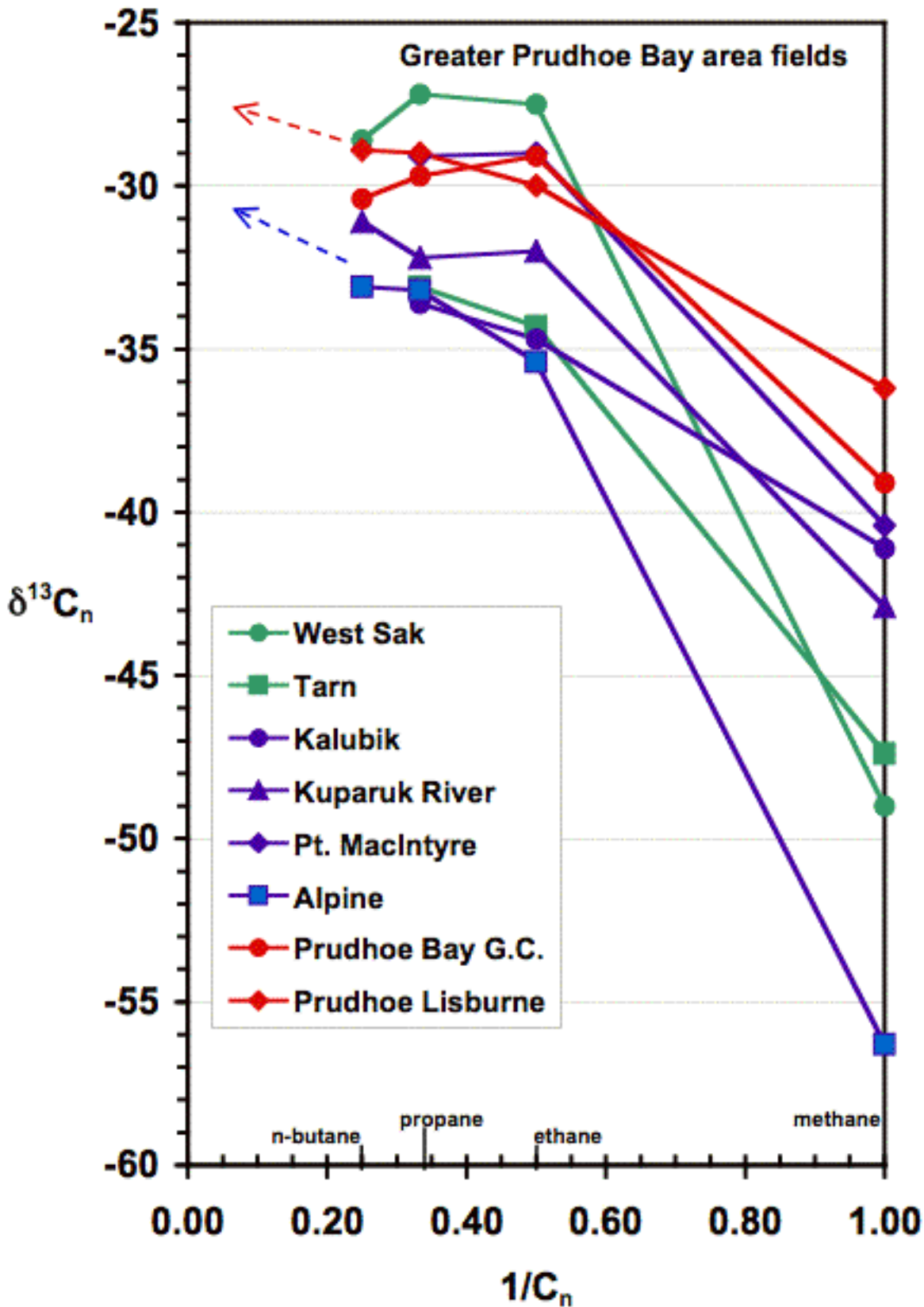


Figure 10. The natural gas plot (Chung, Gormly, and Squires, 1988) showing the carbon isotopic composition of individual hydrocarbons as a function of the carbon number (C_n) of the hydrocarbon. Gases from Walakpa, Wolf Creek, and Umiat fields and one laboratory generated gas from the Hue Shale (see Figure

10E) are shown in 10A. Ranges of the carbon isotopic composition of kerogen from the Shublik Formation, Kingak Shale, Torok Formation shales, and the Pebble shale unit are shown adjacent to the y-axis. Data are from (Burwood, Cole, and others, 1985; Schoell, Wehner, and Coleman, 1985) . Figure 10B shows gases from the South Barrow and East Barrow fields. Gases from the greater Prudhoe Bay area are shown in figure 10C. Additional gases from the greater Prudhoe Bay area and the adjacent fields on the western edge of the greater Kuparuk River field (Masterson, 2001) are shown in 10D. Gases generated in the laboratory during hydrous pyrolysis of North Slope source rocks are shown in Figure 10E. See text for discussion.

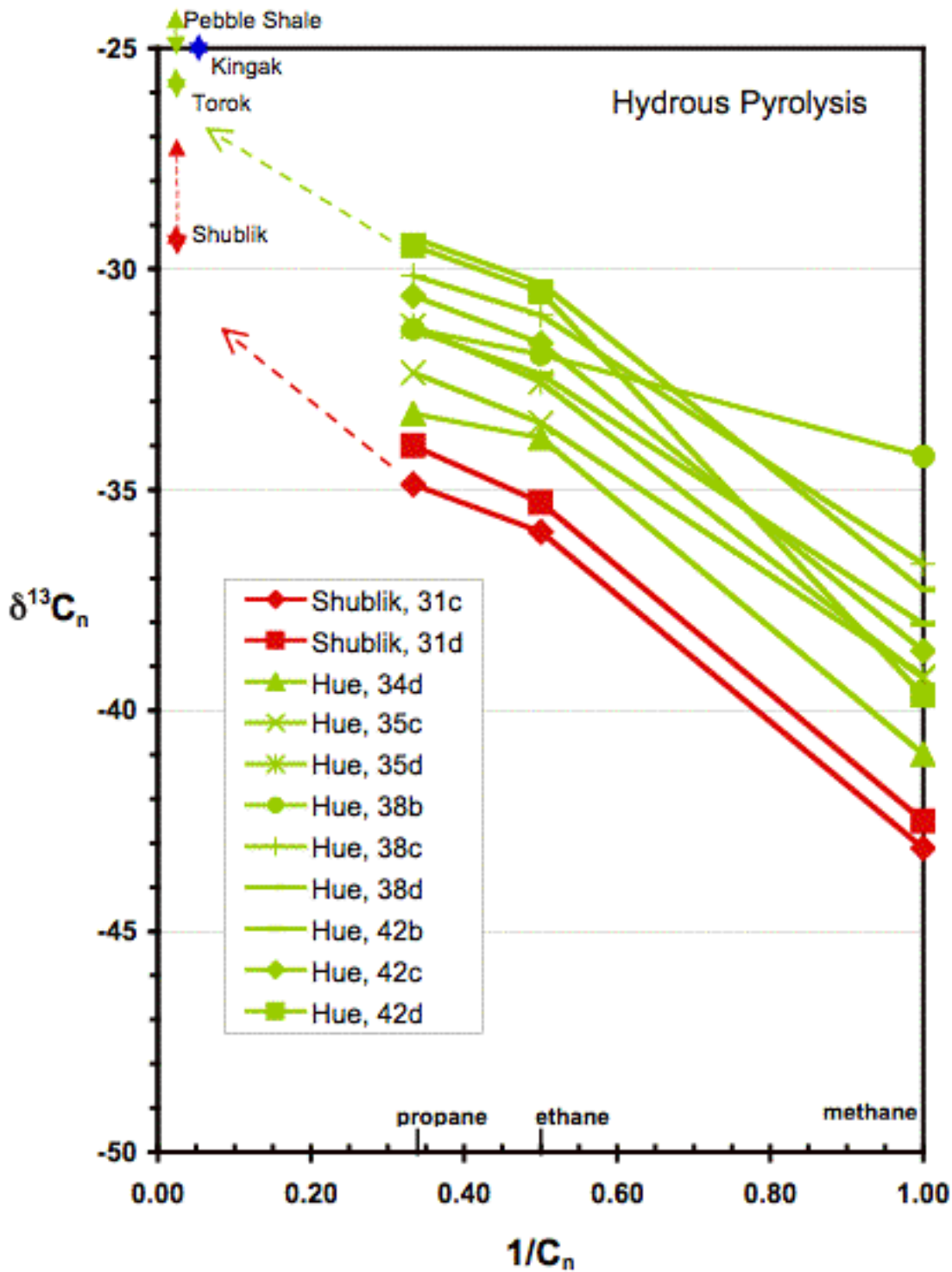


Figure 10. The natural gas plot (Chung, Gormly, and Squires, 1988) showing the carbon isotopic composition of individual hydrocarbons as a function of the carbon number (C_n) of the hydrocarbon. Gases from Walakpa, Wolf Creek, and Umiat fields and one laboratory generated gas from the Hue Shale (see Figure

10E) are shown in 10A. Ranges of the carbon isotopic composition of kerogen from the Shublik Formation, Kingak Shale, Torok Formation shales, and the Pebble shale unit are shown adjacent to the y-axis. Data are from (Burwood, Cole, and others, 1985; Schoell, Wehner, and Coleman, 1985) . Figure 10B shows gases from the South Barrow and East Barrow fields. Gases from the greater Prudhoe Bay area are shown in figure 10C. Additional gases from the greater Prudhoe Bay area and the adjacent fields on the western edge of the greater Kuparuk River field (Masterson, 2001) are shown in 10D. Gases generated in the laboratory during hydrous pyrolysis of North Slope source rocks are shown in Figure 10E. See text for discussion.

Figure 11

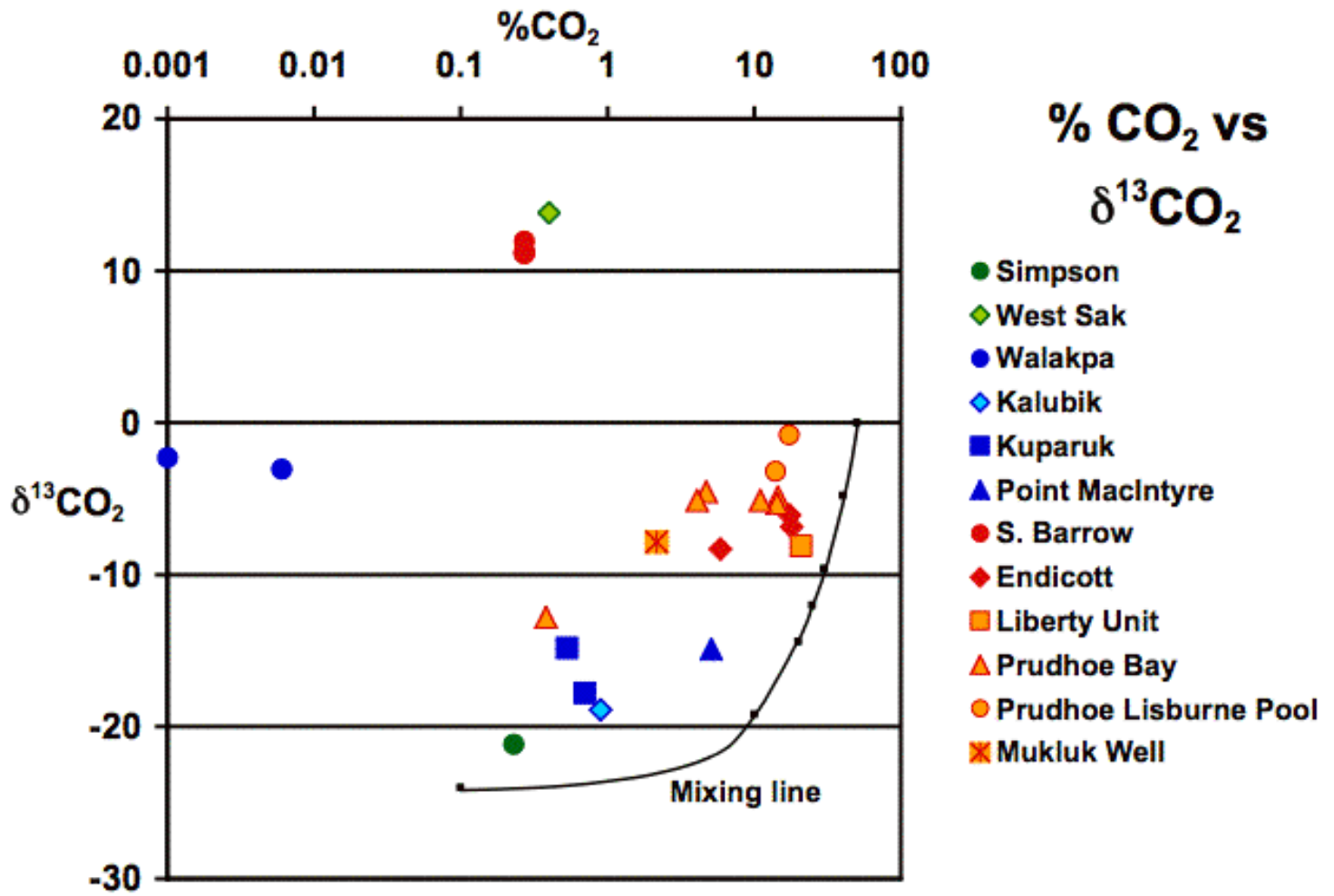


Figure 11. Carbon dioxide concentration as a function of the carbon isotopic composition of CO₂ with samples distinguished by stratigraphic sequence of the reservoir.

Figure 12

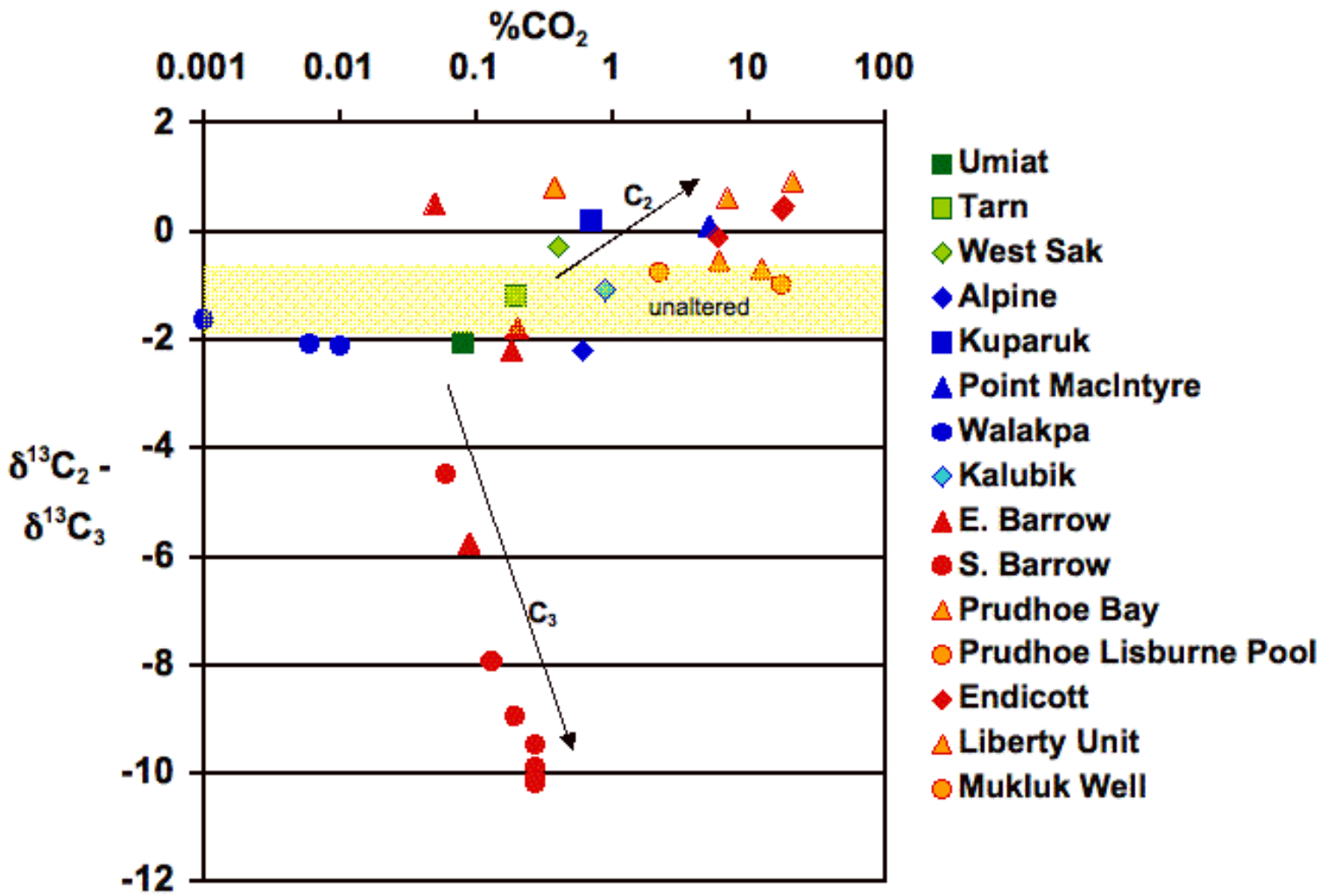


Figure 12. Carbon dioxide concentration as a function of the difference in carbon isotopic composition of ethane (C₂) and propane (C₃). Arrows indicate different paths for gases altered by microbial oxidation of ethane and propane.